



Published in final edited form as:

Acta Neuropathol. 2012 June ; 123(6): 861–872. doi:10.1007/s00401-012-0986-4.

Neuromyelitis optica IgG and natural killer cells produce NMO lesions in mice without myelin loss

Julien Ratelade,

Department of Medicine, University of California, San Francisco, 1246 Health Sciences East Tower, San Francisco, CA 94143-0521, USA

Department of Physiology, University of California, San Francisco, 1246 Health Sciences East Tower, San Francisco, CA 94143-0521, USA

Hua Zhang,

Department of Medicine, University of California, San Francisco, 1246 Health Sciences East Tower, San Francisco, CA 94143-0521, USA

Department of Physiology, University of California, San Francisco, 1246 Health Sciences East Tower, San Francisco, CA 94143-0521, USA

Samira Saadoun,

Academic Neurosurgery Unit, St. George's University of London, London SW17 0RE, UK

Jeffrey L. Bennett,

Department of Neurology, University of Colorado Denver, Aurora, CO 80045, USA

Department of Ophthalmology, University of Colorado Denver, Aurora, CO 80045, USA

Marios C. Papadopoulos, and

Academic Neurosurgery Unit, St. George's University of London, London SW17 0RE, UK

A. S. Verkman

Department of Medicine, University of California, San Francisco, 1246 Health Sciences East Tower, San Francisco, CA 94143-0521, USA Alan.Verkman@ucsf.edu URL: <http://www.ucsf.edu/verklab>

Department of Physiology, University of California, San Francisco, 1246 Health Sciences East Tower, San Francisco, CA 94143-0521, USA

Abstract

The pathogenesis of neuromyelitis optica (NMO) involves targeting of NMO-immunoglobulin G (NMO-IgG) to aquaporin-4 (AQP4) on astrocytes in the central nervous system. Prior work provided evidence for complement-dependent cytotoxicity (CDC) in NMO lesion development. Here, we show that antibody-dependent cellular cytotoxicity (ADCC), in the absence of complement, can also produce NMO-like lesions. Antibody-dependent cellular cytotoxicity was produced in vitro by incubation of mouse astrocyte cultures with human recombinant monoclonal NMO-IgG and human natural killer cells (NK-cells). Injection of NMO-IgG and NK-cells in mouse brain caused loss of AQP4 and GFAP, two characteristic features of NMO lesions, but little myelin loss. Lesions were minimal or absent following injection of: (1) control (non-NMO) IgG with NK-cells; (2) NMO-IgG and NK-cells in AQP4-deficient mice; or (3) NMO-IgG and NK-cells in wild-type mice together with an excess of mutated NMO-IgG lacking ADCC effector

function. NK-cells greatly exacerbated NMO lesions produced by NMO-IgG and complement in an ex vivo spinal cord slice model of NMO, causing marked myelin loss. NMO-IgG can thus produce astrocyte injury by ADCC in a complement-independent and dependent manner, suggesting the potential involvement of ADCC in NMO pathogenesis.

Keywords

NMO; Aquaporin; Natural killer cell; Astrocyte; Demyelination

Introduction

Neuromyelitis optica (NMO) is an inflammatory demyelinating disease of the central nervous system (CNS) primarily affecting optic nerve and spinal cord, and to a lesser extent brain [14, 43]. A defining feature of NMO is the presence in serum of immunoglobulin G autoantibodies (NMO-IgG) targeting aquaporin-4 (AQP4) [15, 16], the major water channel of astrocytes in the CNS [9, 24]. AQP4 is concentrated at the end-feet of astrocytes facing the blood–brain barrier, where it facilitates water exchange between the CNS and the circulation [21].

Though there is an increasing body of evidence that NMO-IgG is pathogenic in NMO [14], the mechanisms by which NMO-IgG produces neuroinflammatory demyelinating lesions are incompletely understood. Antibodies can have several effector functions when bound to their target [8], including (1) modification of target function; (2) target internalization, reducing surface expression; (3) complement activation, causing cell death (complement-dependent cytotoxicity, CDC); and (4) recruitment of effector cells, including natural killer cells, causing cell death (antibody-dependent cellular cytotoxicity, ADCC). NMO-IgG binding to AQP4 does not affect target function—AQP4 water permeability (mechanism 1) [23]. Though NMO-IgG binding causes AQP4 internalization in transfected cell cultures (mechanism 2) [12], there is little AQP4 internalization in primary astrocyte cultures or mouse brain in vivo following NMO-IgG binding [27].

There is strong evidence for involvement of CDC in NMO (mechanism 3) [12, 30]. The Fc region of NMO-IgG binds C1q, causing complement activation and cell lysis [10, 33]. Incubation of AQP4-transfected cells or rat astrocyte cultures with NMO-IgG and complement leads to cell death [10, 33]. Human NMO lesions show a perivascular pattern of activated complement [22]. Intracerebral injection of NMO-IgG and human complement in mice produces NMO-like lesions with perivascular deposition of activated complement, inflammatory cell accumulation, and loss of AQP4, GFAP and myelin [31]. Similar NMO-like pathology is produced by incubation of ex vivo spinal cord slice cultures with NMO-IgG and complement [48]. It is speculated that astrocyte damage triggers an inflammatory cascade with blood–brain barrier breakdown, recruitment of granulocytes and macrophages, and cytokine secretion, resulting in myelin loss and neurological deficit [11, 14, 41].

Natural killer (NK) cells can produce ADCC (mechanism 4) [2]. Antibody-dependent cellular cytotoxicity is exploited in cancer therapy in which tumor cells are targeted by monoclonal antibodies [1]. The antibody Fc region binds CD16 receptors (Fc γ RIII) on NK-cells, leading to their activation and degranulation [1]. Activated NK-cells release cytotoxic granules containing perforin and granzymes that promote apoptosis in target cells. NMO-IgG together with NK-cells can cause death of AQP4-transfected cells and human astrocyte cultures [3, 42]. However, the relevance of ADCC in NMO is not known. Though NK-cells are not seen abundantly in human NMO lesions, their short lifetime following activation precludes any conclusion about their involvement in NMO pathogenesis. However, other

immune cells that can also produce ADCC, including granulocytes, are found abundantly in human NMO lesions and in NMO mouse models [18, 22, 30, 31].

Here, we investigated the potential involvement of ADCC in NMO disease pathogenesis using human recombinant NMO-IgG and human NK-cells in astrocyte cell cultures, mouse brain in vivo (intraparenchymal injection model) [31] and mouse spinal cord slice cultures ex vivo [48]. We show that NMO-IgG and NK-cells can produce astrocyte injury in CNS tissues in a complement-independent manner. NK-cells also exacerbated NMO lesions when complement was present. A competing mutated NMO-IgG that selectively lacks ADCC effector function greatly reduced lesions in mouse brain. These findings have implications for NMO disease pathogenesis.

Materials and methods

Mice

AQP4 null mice used in this study have been described and extensively characterized [19]. Experiments were done on weight-matched wild type and AQP4 null mice on a CD1 genetic background, generally of age 16–18 weeks. The mice were maintained in air-filtered cages and fed normal mouse chow in the UCSF Animal Care Facility. All procedures were approved by the UCSF Committee on Animal Research.

NMO antibodies, DNA constructs

Purified human monoclonal recombinant NMO-IgG rAb-53 was generated as described [3], with a measles virus-specific rAb (2B4) used as an isotype-matched control (control IgG) [4]. Point mutations were introduced into the IgG1 Fc sequence of the rAb-53 heavy chain to produce antibodies selectively lacking ADCC (K326W/E333S, AQmab^{ADCC}) or CDC (K322A, AQmab^{CDC}) [37]. Plasmid pcDNA3.1 encoding the M23 isoform of human AQP4 was generated as described [7].

Cell culture and transfections

Chinese Hamster Ovary (CHO-K1) cells (ATCC CCL-61) were cultured at 37 °C in 5 % CO₂/95 % air in F12 Ham's medium (Sigma-Aldrich, St. Louis, MO) containing 10 % fetal bovine serum (FBS) and 1 % penicillin/streptomycin. The cells were grown on glass coverslips and transfected with DNAs in antibiotic-free medium using Lipofectamine 2000 (Invitrogen, Carlsbad, CA). Stable AQP4-expressing clones were selected following enrichment in Geneticin (Invitrogen) and plating in 96-well plates at low density. Primary astrocyte cultures were generated from cortex of neonatal wild-type and AQP4-null mice, as described [17]. Immunocytochemistry showed that >95 % of cells were positive for the astrocyte marker, glial fibrillary acidic protein (GFAP). Human NK-cells were purchased from Fox Chase Cancer Center (Philadelphia, PA) in which parental NK-92 cells (ATCC CRL-2407) were retrovirally transduced to express the high-affinity 176V variant of the Fc receptor CD16 in pBMN-NoGFP [47] or in pBMN-IRES-EGFP (Invitrogen). NK-cells were cultured in suspension in α -MEM (Sigma-Aldrich) containing 0.1 mM 2-mercaptoethanol, 2 mM L-glutamine, 0.2 mM myoinositol, 10 % FBS, 10 % horse serum, 2.5 μ M folic acid, 5 mL non-essential amino acids (Sigma-Aldrich), 1 mM Na pyruvate, 1 % penicillin/streptomycin, and 100 IU/mL of human recombinant interleukin-2 (Gen-script, Piscataway, NJ).

Complement-dependent cytotoxicity (CDC) and antibody-dependent cellular cytotoxicity (ADCC)

Cells were grown in 24-well (CDC) or 96-well (ADCC) plates until confluence. For assay of CDC, CHO cells expressing human AQP4-M23 or mouse primary astrocyte cultures were

incubated for indicated times with 10 % human complement and 20 $\mu\text{g/ml}$ NMO-IgG or control IgG or AQmab^{ADCC} at 37 °C. Calcein-AM and ethidium-homodimer (Invitrogen) were added to stain live cells green and dead cells red. For assay of ADCC, NK-92 cells expressing CD16 were used as the effector cells. The cells were incubated for 1 h at 37 °C with effector cells and control or NMO-IgG (20 $\mu\text{g/ml}$) at an effector:target cell ratio of 20:1. In some studies 200 $\mu\text{g/ml}$ AQmab^{ADCC} was added. The percentage of dead cells was quantified in five different wells for each condition in two sets of independent experiments (~500 cells counted per well).

Intracerebral injection of NMO-IgG

The mice were anesthetized and mounted on a stereotactic frame. A midline scalp incision was made and a burr hole of diameter 1 mm was drilled in the skull 2 mm to the right of bregma. A 30-gauge needle attached to 50- μL gas-tight glass syringe (Hamilton) was inserted 3-mm deep to infuse 4 μg NMO-IgG (or control IgG) and 10^6 NK-cells in 8 μL PBS (~1 $\mu\text{L/min}$). After 4 days the mice were anesthetized and perfused through the left cardiac ventricle with 5 mL PBS and then 20 mL of PBS containing 4 % paraformaldehyde (PFA). Brains were post-fixed for 2 h in 4 % PFA and processed for paraffin embedding. 5 μm -thick sections were used for immunostaining. In some experiments, 1 μg NMO-IgG was injected with 10^6 NK-cells and 5 μg of AQmab^{ADCC} in a volume of 8 μL . In CDC studies, 0.4 μg NMO-IgG was injected with 3 μL of human complement in a volume of 8 μL .

Immunofluorescence and immunohistochemistry

5 μm -thick paraffin sections were deparaffinized and rehydrated in serial ethanols. Antigen retrieval was performed by incubation of sections in 0.05 % trypsin for 30 min at 37 °C. Tissue sections were immunostained with the following primary antibodies at room temperature for 1 h: rabbit anti-AQP4 (1:200, Santa Cruz Biotechnology, Santa Cruz, CA), mouse anti-GFAP (1:100, Millipore, Temecula, CA), goat anti-myelin basic protein (MBP) (1:200, Santa Cruz Biotechnology), rabbit anti-Iba1 (1:500, Wako, Richmond, VA), rat anti-CD45 (1:10, Pharmingen, BD Biosciences, Oxford, UK), rat anti-macrophage (F4/80 antigen) (1:10, eBioscience, Hatfield, UK), rat anti-neutrophil (GR-1 antibody) (1:10, eBioscience) or rabbit anti-C5b-9 (1:50, Santa Cruz Biotechnology) followed by the appropriate species-specific biotinylated secondary antibody (1:500, Vector Laboratories) or Alexa Fluor-conjugated secondary antibody (1:200, Invitrogen). When biotinylated secondary antibody was used, immunostaining was visualized as brown using the Vectastain horseradish peroxidase kit (Vector Laboratories) followed by diaminobenzidine/ H_2O_2 according to manufacturer's protocol. Nuclei were counterstained blue with hematoxylin. Tissue sections were examined with a Leica DM 4000 B microscope. Lesions were quantified by imaging at 2.5 \times magnification. AQP4, GFAP, and MBP immunonegative areas were defined by hand and quantified using ImageJ (version 1.43 m, National Institutes of Health, USA; <http://rsbweb.nih.gov/ij>). Data are presented as percentage of immunonegative area (normalized to total area of hemi-brain slice).

Ex vivo NMO model

Organotypic spinal cord slice cultures were prepared using a modified interface-culture method as described [48]. In brief, postnatal day 7 mouse pups were decapitated and the spinal cord was rapidly removed and placed in ice-cold Hank's balanced salt solution (HBSS, pH 7.2, Invitrogen). Transverse slices of cervical spinal cord of thickness 300 μm were cut using a vibratome (VT-1000S; Leica, Wetzlar, Germany). Individual slices were placed on transparent, non-coated membrane inserts (Millipore, Millicell-CM 0.4 μm pores, 30 mm diameter) in six-well (35 mm diameter) plates containing 1 mL culture medium, with a thin film of culture medium (50 % MEM, 25 % HBSS, 25 % horse serum, 1 % penicillin-streptomycin, 0.65 % glucose, and 25 mM HEPES) covering slices. Slices were cultured in

5 % CO₂ at 37 °C for 7 days. At day 7, NMO-IgG, NK-cells or human complement were added to both sides of the porous membrane, with 1 mL medium added above the porous filter to fully immerse the slice. After 24 h, slice cultures were fixed in 4 % PFA for 15 min and incubated in blocking solution (PBS containing 1 % BSA and 0.3 % Triton X-100) for 1 h. The slices were then incubated for 2 h with antibodies against mouse GFAP (1:1000, Millipore), AQP4 (1:200, Millipore), Iba1 (1:1000, Wako) or MBP (1:100, Santa Cruz Biotechnology), rinsed in PBS, and then incubated with secondary antibodies for 1 h at room temperature. Immunofluorescence was visualized on a Leica DM 4000 B microscope. AQP4- and GFAP-stained spinal cord slices were scored for lesion severity using the following scale: 0, intact slice with intact GFAP and AQP4 staining; 1, intact slice with some astrocyte swelling (seen from GFAP stain) with weak AQP4 staining; 2, at least one lesion with complete loss of GFAP and AQP4 staining; 3, multiple lesions with loss of GFAP and AQP4 staining in >30 % of slice area; and 4, extensive loss of GFAP and AQP4 staining affecting >80 % of slice area. AQP4 null slices were scored only on the basis of GFAP staining.

Statistics

Data are presented as mean ± SEM. Statistical comparisons were made using the non-parametric Mann–Whitney test when comparing two groups.

Results

NMO-IgG and NK-cells produce ADCC in primary astrocyte cultures

We previously demonstrated that the recombinant monoclonal NMO-IgG rAb-53 binds rapidly and with high affinity to native AQP4 expressed on primary cultures of mouse astrocytes [28]. For studies of CDC and ADCC in mouse CNS tissues, we first verified that the recombinant NMO-IgG can produce cytotoxicity in mouse astrocyte cultures. As a positive control, we used CHO cells transfected with the M23 isoform of human AQP4 (CHO-M23). Incubation of CHO-M23 cultures with NMO-IgG (20 µg/ml) and 10 % human complement for 30 min caused cytotoxicity as visualized by a live/dead cell assay in which live cells are stained green and dead cells red (48 ± 1 % dead cells, SE, $n = 5$) (Fig. 1a). No cytotoxicity was seen with NMO-IgG alone or with control (non-NMO) IgG and complement, or in non-transfected CHO cells incubated with NMO-IgG and complement. A mutated NMO-IgG deficient in ADCC effector function, AQmab^{ADCC}, also caused cytotoxicity (42 ± 4 % dead cells, $n = 5$) when added with complement, as CDC effector function is preserved in this antibody. Under the same conditions, NMO-IgG and complement caused little cytotoxicity on mouse primary astrocytes after a 30 min incubation (not shown). Significant cytotoxicity was seen, however, after 3 h with NMO-IgG (68 ± 1 % dead cells, $n = 5$) or AQmab^{ADCC} (54 ± 8 % dead cells, $n = 5$).

Figure 1b shows cytotoxicity in CHO-M23 cells incubated with NMO-IgG and human NK-cells for 1 h (33 ± 3 % dead cells, $n = 5$). Minimal cell killing was seen with NK-cells and control IgG, when NK-cells and NMO-IgG were added in the presence of an excess of AQmab^{ADCC}, or when NK-cells and NMO-IgG were incubated with non-transfected CHO cells. In contrast to the CDC results, after the same incubation time (1 h) marked cytotoxicity was found in primary cultures of mouse astrocytes incubated with NMO-IgG and NK-cells (50 ± 5 % dead cells, $n = 5$). Little or no ADCC was found in controls (NK-cells and control IgG; NK-cells and NMO-IgG with excess of AQmab^{ADCC}; NMO-IgG and NK-cells in AQP4 null astrocytes).

Intracerebral injection of NMO-IgG and NK-cells causes astrocyte injury

Injection of NMO-IgG (purified IgG from NMO serum) and human complement in mouse brain produces inflammatory demyelinating lesions [31]. Here, ADCC was studied in vivo by a similar approach involving intracerebral injection of recombinant NMO-IgG and human NK-cells. At 4 days after injection brain sections were stained for astrocyte and oligodendrocyte markers. Figure 2a shows marked loss of AQP4 and GFAP immunoreactivity in the region of the injection site. Reactive gliosis, with increased GFAP immunoreactivity (compared to contralateral hemisphere) was seen around the lesion (Fig. 2a, b). Interestingly, staining for myelin basic protein (MBP) was not reduced, suggesting preservation of oligodendrocytes. In the non-injected hemisphere, AQP4 staining was seen mainly in a perivascular pattern in astrocyte end-feet, with weak GFAP immunofluorescence in astrocyte cell bodies. Minimal loss of AQP4 and GFAP was seen when NK-cells were injected with control IgG. Minimal loss of GFAP was seen when NMO-IgG and NK-cells were injected in AQP4-deficient mice. In these controls, upregulation of GFAP was generally seen around the needle tract, suggesting non-specific reactive gliosis due to the needle insertion. Figure 2c summarizes areas of loss of AQP4, GFAP and myelin immunoreactivity. While NMO-IgG and NK-cells caused significant loss of AQP4 and GFAP, no significant loss of myelin was found. These results indicate that astrocyte injury in vivo can be produced by NK-cell action on NMO-IgG bound to AQP4.

Infiltrating CD45-positive cells were seen along the needle tract, both in test and control mice, suggesting non-specific inflammation related to the needle insertion (Fig. 3a). These cells were identified as macrophages by staining with a specific antibody. Iba1 staining showed few microglia with small soma and fine cellular processes in the contralateral hemisphere, but many activated microglia with bigger cell bodies around the needle track (Fig. 3b). However, microglial activation was comparable in test and control mice, suggesting that astrocyte damage by NK-cells in our model does not involve microglial activation.

We previously showed that NMO-IgG can diffuse over a relatively large area [28], substantially greater than size of the ADCC lesion here. We postulated that the relatively small lesion size is related to restricted NK-cell diffusion. NK-cell localization was studied by intracerebral injection of GFP-labeled NK-cells. After 24 h, NK-cell density was ~150 cells/mm² within 400 μm from the needle tract (Fig. 3c) with cells seen up to 700 μm from the needle tract, which approximately corresponds to the extent of the lesion. After 4 days, few remaining GFP-positive cells were seen in the brain parenchyma away from the needle track, suggesting that these cells are short-lived and that NK-cell-dependent ADCC is an early process.

Astrocyte injury produced by NMO-IgG and NK-cells is mediated by ADCC in a complement-independent manner

To confirm that ADCC is responsible for astrocyte injury following injection of NMO-IgG and NK-cells, the ADCC-deficient mutant AQmab^{ADCC} was coinjected at a five-fold excess over NMO-IgG. Figure 4a shows significantly reduced areas of AQP4 and GFAP loss with AQmab^{ADCC}, as quantified in Fig. 4b. Lesion areas were smaller in this study compared to Fig. 2c (18 % vs. 43 % for AQP4 loss) because four-fold less NMO-IgG was injected (to allow injection of excess AQmab^{ADCC}). As AQmab^{ADCC} is able to mediate ADCC, as shown in Fig. 1a, we conclude that ADCC is responsible for the NMO-IgG/NK-cell dependent lesions in this model. Also, we verified that complement activation was not involved by absence of C5b-9 antibody staining (Fig. 4c).

NMO-IgG-dependent lesions produced by ADCC versus CDC are different

We compared the lesions caused by ADCC and CDC in the intracerebral injection model. To produce CDC, the brains were injected with NMO-IgG and human complement (in place of NK-cells). The brain sections were examined at 4 days after injection. There was marked loss of AQP4 and GFAP, as found in the ADCC model (Fig. 5a, b). However, in contrast to the ADCC model, the CDC model produced marked myelin loss, suggesting injury to both astrocytes and oligodendrocytes. Marked CD45-positive cell infiltration was observed in the lesion in the CDC model (Fig. 5c). Most of the infiltrating cells were stained with a macrophage-specific antibody but were negative for a neutrophil marker. We also found perivascular deposition of activated complement in this model (Fig. 5d).

NK-cells exacerbate lesions caused by NMO-IgG and complement

Studies were also done to determine whether NK-cells could exacerbate lesions produced by NMO-IgG and complement. These studies were done using ex vivo spinal cord slice cultures in order to control the exact amount of NMO-IgG, complement and NK-cells, and to obviate issues of differential antibody and cell diffusion in vivo. To test whether NK-cells could produce NMO pathology in spinal cord slices in the absence of complement, NK-cells (10^6 /well) were added to slice cultures for 24 h together with NMO-IgG ($10 \mu\text{g/mL}$). Figure 6a shows marked loss of GFAP and AQP4 staining in slices exposed to NK-cells and NMO-IgG, which was not seen with in their absence (control), with NK-cells alone, or in slices from AQP4 knockout mice. AqMab^{ADCC} ($10 \mu\text{g/mL}$) did not cause NK-cell dependent pathology, whereas AqMab^{CDC} (mutated NMO-IgG selectively lacking CDC) did.

Though NK-cells do not participate directly in CDC, we found that they can exacerbate complement-dependent NMO lesions. Figure 6b shows that addition of human complement (5 %) and submaximal NMO-IgG ($3 \mu\text{g/mL}$) produced very mild lesions, as did NK-cells (10^6 /well) with submaximal NMO-IgG ($3 \mu\text{g/mL}$). However, addition of NK-cells together with human complement and submaximal NMO-IgG consistently produced severe lesions (scores summarized in Fig. 6b right) with marked myelin loss.

Discussion

Complement-dependent pathogenicity of NMO-IgG has been described in astrocyte cultures, in mouse brain in vivo, and in ex vivo cultures of spinal cord and optic nerve. In human NMO lesions perivascular deposition of activated complement is prominent. Here, we investigated the potential involvement of ADCC in NMO pathogenesis. We found: (1) NMO-IgG together with NK-cells causes astrocyte cytotoxicity in cultures; (2) NMO-IgG and NK-cells cause astrocyte injury in brain in vivo, characterized by loss of AQP4 and GFAP; (3) NMO-IgG mediated ADCC in the absence of complement causes minimal myelin loss and inflammation compared to lesions caused by NMO-IgG and complement; and (4) NK-cells greatly exacerbate NMO lesions caused by NMO-IgG and complement in ex vivo spinal cord slices.

Efficient cytotoxicity was found in astrocyte cultures exposed to NMO-IgG and NK-cells. We found comparable susceptibility to ADCC in primary astrocyte cultures and AQP4-transfected cells. In contrast, astrocytes were much less sensitive to CDC than AQP4-transfected cells, which is likely the consequence of complement inhibitor proteins, including CD55 which accelerates decay of C3 convertases, and CD59 which inhibits the membrane attack complex on host cells [20]. These complement inhibitors are expressed in astrocytes in human brain and in rodent primary cultures [35, 46]. Importantly, these complement inhibitor proteins protect against CDC but not ADCC. Also, we recently showed that CDC, but not ADCC, requires AQP4 assembly in orthogonal arrays of particles

[25], providing a second mechanism of enhanced susceptibility to ADCC versus CDC in AQP4-expressing target cells.

Antibody-dependent cellular cytotoxicity was investigated *in vivo* by direct intraparenchymal injection of NMO-IgG and NK-cells into mouse brain. There was marked loss of AQP4 and GFAP at 4 days, which are two characteristic features of human NMO lesions [22] and of lesions in mouse brain injected with NMO-IgG and complement [31]. The loss of GFAP and AQP4 is likely caused by astrocyte damage and death, as binding of NK-cells to the Fc portion of AQP4-bound NMO-IgG causes NK-cell degranulation and killing of target cells. Minimal or no loss of GFAP or AQP4 were found in key control experiments, including injection of control (non-NMO) antibody and NK-cells, and injection of NMO-IgG and NK-cells in AQP4-deficient mice. Injection of NMO-IgG and NK-cells in wild-type mice together with an excess of a mutant NMO-IgG lacking ADCC effector function greatly reduced GFAP and AQP4 loss, indicating ADCC as the pathogenic mechanism in this model. These results thus describe the first complement-independent *in vivo* model of NMO. Our findings suggest the potential utility in NMO of mutant NMO-IgG lacking both CDC and ADCC effector functions (aquaporumab) [37] and small-molecule blockers of NMO-IgG binding to AQP4 [36].

The NK-92 cell line used in this study was transfected with the Fc receptor CD16 containing an allelic polymorphism at residue 176, with substitution of the phenylalanine (F) at this position for valine (V). NK-cells from individuals homozygous for the V substitution bind higher levels of IgG1 and IgG3 than those homozygous for F at this position [44]. The F variant, which represents 56 % of all alleles in the human population, is also able to produce ADCC but with lower efficiency than the V variant [40]. Therefore, polymorphisms in the CD16 gene may potentially influence NMO lesion severity due to their effects on ADCC. The frequency of CD16 176V substitution in the NMO patient population has not been evaluated.

A resident cell type in the human CNS expressing Fc receptors is microglia, which has been reported to mediate ADCC *in vitro* [38]. We found similar microglial cell activation and migration around the needle tract following injection of NK-cells and either NMO-IgG or control antibody, suggesting that microglia-induced ADCC does not occur in our model. Activation of microglia around a stab injury is well described [29]. The lack of involvement of microglia in our model is supported by the absence of lesions following injection of NMO-IgG alone [28, 31].

A remarkable difference in lesions produced by injection of NMO-IgG and NK-cells (ADCC model) versus injection of NMO-IgG and complement (CDC model) is the relative preservation of myelin in the ADCC model. In contrast to multiple sclerosis, in NMO it is thought that primary astrocyte injury produced by NMO-IgG secondarily injures oligodendrocytes leading to demyelination [22]. NMO lesions have been reported with prominent loss of AQP4 and GFAP, but preservation of myelin [22], suggesting that demyelination is a secondary process. It is not known whether oligodendrocyte injury in NMO is a bystander reaction of the inflammatory process, a consequence of the toxicity of activated complement components, or a specific disturbance of the homeostatic interaction between astrocytes and oligodendrocytes.

Another remarkable difference between the ADCC and CDC models is the massive infiltration of inflammatory cells in the CDC model. By immunostaining at 4 days after injection, we identified the inflammatory cells as mainly macrophages. At earlier time points there is evidence for marked accumulation of neutrophils as well in this model [32]. Activation of the complement cascade involves the release of soluble factors, including the

anaphylatoxins C3a and C5a, which have proinflammatory and chemotactic actions [45]. The ability of complement to recruit cells of the immune system may explain the marked difference in inflammation found in the CDC versus ADCC models. Our findings also suggest that demyelination in NMO may be related to infiltration of inflammatory cells, as myelin loss was minimal in the ADCC model.

We also demonstrated that NMO-IgG and NK-cells cause astrocyte damage with little myelin loss in an ex vivo spinal cord slice model. As found in brain in vivo, the pathogenic mechanism involved is ADCC, as Aqumab^{ADCC} and NK-cells did not produce lesions. Interestingly, we found marked synergy between NK-cells, complement and NMO-IgG in producing astrocyte damage and myelin loss in spinal cord slices. This synergy is probably accounted for by “complement-mediated cell cytotoxicity” in which complement recruitment and activation at the surface of target cells facilitates binding of effector cells [26].

NK-cells comprise 10–20 % of human peripheral blood lymphocytes and are believed to be the main effector cells in cancer therapy involving monoclonal antibodies targeting tumor cells [6]. Antibodies targeting CD20, Her2/neu, epidermal growth factor receptor and disialoganglioside are examples of clinically successful antibodies that exploit NK-cell-mediated ADCC to kill tumor cells. Although NK-cells are not prominent in human NMO lesions, this might be related to their short lifetime after migration into the CNS, as they rapidly degranulate and die upon binding to the Fc portion of NMO-IgG [2]. Indeed, we found here that the vast majority of injected fluorescent NK-cells in mouse brain disappeared after 4 days.

Multiple leukocyte types besides NK-cells can participate in ADCC. NMO-IgG in NMO is predominantly of the IgG1 subtype, which is able to bind all classes of Fc receptors involved in ADCC [5]. Several leukocyte types express Fc receptors, including macrophages, which express the three classes of Fc receptors FcγRI (CD64), FcγRII (CD32) and FcγRIII (CD16), and neutrophils and eosinophils, which express FcγRII and FcγRIII [5]. It has been reported that these cell types can mediate ADCC in vivo [13, 34, 39]. Since granulocytes and macrophages are generally found in NMO lesions, they may also contribute to the pathogenesis of NMO lesions by an ADCC mechanism. We reported in spinal cord slice cultures that macrophages and neutrophils exacerbate NMO lesions caused by submaximal NMO-IgG and complement, which probably involves an ADCC mechanism [48]. It is likely that these immune cells mediate CNS injury through FcR-mediated release of proteases, elastases, reactive oxygen species, and nitrous oxide. We reported recently that inhibition of neutrophil proteases with Sivelestat and cathepsin G inhibitor 1 reduced NMO lesions in the murine intracerebral injection model [32]. In the study here we used NK-cells as proof of concept to demonstrate that NMO-IgG-driven ADCC in vivo can produce NMO-like lesions. Though our data suggest the involvement of ADCC in NMO, definitive quantification of ADCC in human NMO would require a clinical trial involving administration of an aquaporin deficient for the ADCC function, or, if it can be developed, a selective inhibitor of ADCC.

In conclusion, our data suggest the potential involvement of ADCC in NMO disease pathogenesis, as a second disease mechanism in addition to the well-characterized role of CDC. Also, our mouse model of NMO-IgG and NK-cell exposure provides an interesting tool to study the biology of astrocyte damage and demyelination.

Acknowledgments

This work was supported by grants from the Guthy-Jackson Charitable Foundation (ASV, MCP, JLB), Grants EY13574, EB00415, DK35124, HL73856, DK86125 and DK72517 from the National Institutes of Health (ASV) and grant RG4320 from the National Multiple Sclerosis Society (JLB).

References

1. Alderson KL, Sondel PM. Clinical cancer therapy by NK cells via antibody-dependent cell-mediated cytotoxicity. *J Biomed Biotechnol.* 2011; 2011:379123. [PubMed: 21660134]
2. Becknell B, Caligiuri MA. Natural killer cells in innate immunity and cancer. *J Immunother.* 2008; 31(8):685–692. [PubMed: 18779751]
3. Bennett JL, Lam C, Kalluri SR, Saikali P, Bautista K, Dupree C, Glogowska M, Case D, Antel JP, Owens GP, Gilden D, Nessler S, Stadelmann C, Hemmer B. Intrathecal pathogenic anti-aquaporin-4 antibodies in early neuromyelitis optica. *Ann Neurol.* 2009; 66(5):617–629. [PubMed: 19938104]
4. Burgoon MP, Williamson RA, Owens GP, Ghausi O, Bastidas RB, Burton DR, Gilden DH. Cloning the antibody response in humans with inflammatory CNS disease: isolation of measles virus-specific antibodies from phage display libraries of a subacute sclerosing panencephalitis brain. *J Neuroimmunol.* 1999; 94(1–2):204–211. [PubMed: 10376954]
5. Capel PJ, van de Winkel JG, van den Herik-Oudijk IE, Verbeek JS. Heterogeneity of human IgG Fc receptors. *Immunomethods.* 1994; 4(1):25–34. [PubMed: 8069524]
6. Chiorean EG, Miller JS. The biology of natural killer cells and implications for therapy of human disease. *J Hematother Stem Cell Res.* 2001; 10(4):451–463. [PubMed: 11522229]
7. Crane JM, Verkman AS. Determinants of aquaporin-4 assembly in orthogonal arrays revealed by live-cell single-molecule fluorescence imaging. *J Cell Sci.* 2009; 122(Pt 6):813–821. [PubMed: 19240114]
8. Diamond B, Huerta PT, Mina-Osorio P, Kowal C, Volpe BT. Losing your nerves? Maybe it's the antibodies. *Nat Rev Immunol.* 2009; 9(6):449–456. [PubMed: 19424277]
9. Frigeri A, Gropper MA, Umenishi F, Kawashima M, Brown D, Verkman AS. Localization of MIWC and GLIP water channel homologs in neuromuscular, epithelial and glandular tissues. *J Cell Sci.* 1995; 108(Pt 9):2993–3002. [PubMed: 8537439]
10. Hinson SR, McKeon A, Fryer JP, Apiwatanakul M, Lennon VA, Pittock SJ. Prediction of neuromyelitis optica attack severity by quantitation of complement-mediated injury to aquaporin-4-expressing cells. *Arch Neurol.* 2009; 66(9):1164–1167. [PubMed: 19752309]
11. Hinson SR, McKeon A, Lennon VA. Neurological autoimmunity targeting aquaporin-4. *Neuroscience.* 2010; 168(4):1009–1018. [PubMed: 19699271]
12. Hinson SR, Pittock SJ, Lucchinetti CF, Roemer SF, Fryer JP, Kryzer TJ, Lennon VA. Pathogenic potential of IgG binding to water channel extracellular domain in neuromyelitis optica. *Neurology.* 2007; 69(24):2221–2231. [PubMed: 17928579]
13. Hubert P, Heitzmann A, Viel S, Nicolas A, Sastre-Garau X, Oppezio P, Pritsch O, Osinaga E, Amigorena S. Antibody-dependent cell cytotoxicity synapses form in mice during tumor-specific antibody immunotherapy. *Cancer Res.* 2011; 71(15):5134–5143. [PubMed: 21697279]
14. Jarius S, Wildemann B. AQP4 antibodies in neuromyelitis optica: diagnostic and pathogenetic relevance. *Nat Rev Neurol.* 2010; 6(7):383–392. [PubMed: 20639914]
15. Lennon VA, Kryzer TJ, Pittock SJ, Verkman AS, Hinson SR. IgG marker of optic-spinal multiple sclerosis binds to the aquaporin-4 water channel. *J Exp Med.* 2005; 202(4):473–477. [PubMed: 16087714]
16. Lennon VA, Wingerchuk DM, Kryzer TJ, Pittock SJ, Lucchinetti CF, Fujihara K, Nakashima I, Weinshenker BG. A serum autoantibody marker of neuromyelitis optica: distinction from multiple sclerosis. *Lancet.* 2004; 364(9451):2106–2112. [PubMed: 15589308]
17. Li L, Zhang H, Varrin-Doyer M, Zamvil SS, Verkman AS. Proinflammatory role of aquaporin-4 in autoimmune neuroinflammation. *FASEB J.* 2011; 25(5):1556–1566. [PubMed: 21257712]
18. Lucchinetti CF, Mandler RN, McGavern D, Bruck W, Gleich G, Ransohoff RM, Trebst C, Weinshenker B, Wingerchuk D, Parisi JE, Lassmann H. A role for humoral mechanisms in the

- pathogenesis of Devic's neuromyelitis optica. *Brain*. 2002; 125(Pt 7):1450–1461. [PubMed: 12076996]
19. Ma T, Yang B, Gillespie A, Carlson EJ, Epstein CJ, Verkman AS. Generation and phenotype of a transgenic knockout mouse lacking the mercurial-insensitive water channel aquaporin-4. *J Clin Invest*. 1997; 100(5):957–962. [PubMed: 9276712]
 20. Makrides SC. Therapeutic inhibition of the complement system. *Pharmacol Rev*. 1998; 50(1):59–87. [PubMed: 9549758]
 21. Manley GT, Fujimura M, Ma T, Noshita N, Filiz F, Bollen AW, Chan P, Verkman AS. Aquaporin-4 deletion in mice reduces brain edema after acute water intoxication and ischemic stroke. *Nat Med*. 2000; 6(2):159–163. [PubMed: 10655103]
 22. Misu T, Fujihara K, Kakita A, Konno H, Nakamura M, Watanabe S, Takahashi T, Nakashima I, Takahashi H, Itoyama Y. Loss of aquaporin 4 in lesions of neuromyelitis optica: distinction from multiple sclerosis. *Brain*. 2007; 130(Pt 5):1224–1234. [PubMed: 17405762]
 23. Nicchia GP, Mastrototaro M, Rossi A, Pisani F, Tortorella C, Ruggieri M, Lia A, Trojano M, Frigeri A, Svelto M. Aquaporin-4 orthogonal arrays of particles are the target for neuromyelitis optica autoantibodies. *Glia*. 2009; 57(13):1363–1373. [PubMed: 19229993]
 24. Nielsen S, Nagelhus EA, Amiry-Moghaddam M, Bourque C, Agre P, Ottersen OP. Specialized membrane domains for water transport in glial cells: high-resolution immunogold cytochemistry of aquaporin-4 in rat brain. *J Neurosci*. 1997; 17(1):171–180. [PubMed: 8987746]
 25. Phuan PW, Ratelade J, Rossi A, Tradtrantip L, Verkman AS. Complement-dependent cytotoxicity in neuromyelitis optica requires aquaporin-4 assembly in orthogonal arrays. *J Biol Chem*. 2012; 287:13829–13839. [PubMed: 22393049]
 26. Ramos OF, Nilsson B, Nilsson K, Eggertsen G, Yefenof E, Klein E. Elevated NK-mediated lysis of Raji and Daudi cells carrying fixed iC3b fragments. *Cell Immunol*. 1989; 119(2):459–469. [PubMed: 2522826]
 27. Ratelade J, Bennett JL, Verkman AS. Evidence against cellular internalization in vivo of NMO-IgG, aquaporin-4, and excitatory amino acid transporter 2 in neuromyelitis optica. *J Biol Chem*. 2011; 286(52):45156–45164. [PubMed: 22069320]
 28. Ratelade J, Bennett JL, Verkman AS. Intravenous neuromyelitis optica autoantibody in mice targets aquaporin-4 in peripheral organs and area postrema. *PLoS ONE*. 2011; 6(11):e27412. [PubMed: 22076159]
 29. Robel S, Bardehle S, Lepier A, Brakebusch C, Gotz M. Genetic deletion of *cdc42* reveals a crucial role for astrocyte recruitment to the injury site in vitro and in vivo. *J Neurosci*. 2011; 31(35):12471–12482. [PubMed: 21880909]
 30. Roemer SF, Parisi JE, Lennon VA, Benarroch EE, Lassmann H, Bruck W, Mandler RN, Weinschenker BG, Pittock SJ, Wingerchuk DM, Lucchinetti CF. Pattern-specific loss of aquaporin-4 immunoreactivity distinguishes neuromyelitis optica from multiple sclerosis. *Brain*. 2007; 130(Pt 5):1194–1205. [PubMed: 17282996]
 31. Saadoun S, Waters P, Bell BA, Vincent A, Verkman AS, Papadopoulos MC. Intra-cerebral injection of neuromyelitis optica immunoglobulin G and human complement produces neuromyelitis optica lesions in mice. *Brain*. 2010; 133(Pt 2):349–361. [PubMed: 20047900]
 32. Saadoun S, Waters P, Macdonald C, Bell BA, Vincent A, Verkman AS, Papadopoulos MC. Neutrophil protease inhibition reduces neuromyelitis optica-immunoglobulin G-induced damage in mouse brain. *Ann Neurol*. 2012; 71(3):323–333. [PubMed: 22374891]
 33. Sabater L, Giralt A, Boronat A, Hankiewicz K, Blanco Y, Llufrui S, Alberch J, Graus F, Saiz A. Cytotoxic effect of neuromyelitis optica antibody (NMO-IgG) to astrocytes: an in vitro study. *J Neuroimmunol*. 2009; 215(1–2):31–35. [PubMed: 19695715]
 34. Siders WM, Shields J, Garron C, Hu Y, Boutin P, Shankara S, Weber W, Roberts B, Kaplan JM. Involvement of neutrophils and natural killer cells in the anti-tumor activity of alemtuzumab in xenograft tumor models. *Leuk Lymphoma*. 2010; 51(7):1293–1304. [PubMed: 20377308]
 35. Singhrao SK, Neal JW, Rushmere NK, Morgan BP, Gasque P. Differential expression of individual complement regulators in the brain and choroid plexus. *Lab Invest*. 1999; 79(10):1247–1259. [PubMed: 10532588]

36. Tradtrantip L, Zhang H, Anderson MO, Saadoun S, Phuan PW, Papadopoulos MC, Bennett JL, Verkman AS. Small-molecule inhibitors of NMO-IgG binding to aquaporin-4 reduce astrocyte cytotoxicity in neuromyelitis optica. *FASEB J.* 2012 doi: 10.1096/fj.11-201608.
37. Tradtrantip L, Zhang H, Saadoun S, Phuan PW, Lam C, Papadopoulos MC, Bennett JL, Verkman AS. Anti-aquaporin-4 monoclonal antibody blocker therapy for neuromyelitis optica. *Ann Neurol.* 2012; 71(3):314–322. [PubMed: 22271321]
38. Ulvestad E, Williams K, Matre R, Nyland H, Olivier A, Antel J. Fc receptors for IgG on cultured human microglia mediate cytotoxicity and phagocytosis of antibody-coated targets. *J Neuropathol Exp Neurol.* 1994; 53(1):27–36. [PubMed: 8301317]
39. Valerius T, Repp R, Kalden JR, Platzer E. Effects of IFN on human eosinophils in comparison with other cytokines. A novel class of eosinophil activators with delayed onset of action. *J Immunol.* 1990; 145(9):2950–2958. [PubMed: 1698867]
40. Vance BA, Huizinga TW, Wardwell K, Guyre PM. Binding of monomeric human IgG defines an expression polymorphism of Fc gamma RIII on large granular lymphocyte/natural killer cells. *J Immunol.* 1993; 151(11):6429–6439. [PubMed: 8245476]
41. Verkman AS, Ratelade J, Rossi A, Zhang H, Tradtrantip L. Aquaporin-4: orthogonal array assembly, CNS functions, and role in neuromyelitis optica. *Acta Pharmacol Sin.* 2011; 32(6):702–710. [PubMed: 21552296]
42. Vincent T, Saikali P, Cayrol R, Roth AD, Bar-Or A, Prat A, Antel JP. Functional consequences of neuromyelitis optica-IgG astrocyte interactions on blood-brain barrier permeability and granulocyte recruitment. *J Immunol.* 2008; 181(8):5730–5737. [PubMed: 18832732]
43. Wingerchuk DM, Lennon VA, Lucchinetti CF, Pittock SJ, Weinshenker BG. The spectrum of neuromyelitis optica. *Lancet Neurol.* 2007; 6(9):805–815. [PubMed: 17706564]
44. Wu J, Edberg JC, Redecha PB, Bansal V, Guyre PM, Coleman K, Salmon JE, Kimberly RP. A novel polymorphism of Fc gamma RIIIa (CD16) alters receptor function and predisposes to autoimmune disease. *J Clin Invest.* 1997; 100(5):1059–1070. [PubMed: 9276722]
45. Yanamadala V, Friedlander RM. Complement in neuro-protection and neurodegeneration. *Trends Mol Med.* 2010; 16(2):69–76. [PubMed: 20116331]
46. Yang C, Jones JL, Barnum SR. Expression of decay-accelerating factor (CD55), membrane cofactor protein (CD46) and CD59 in the human astrogloma cell line, D54-MG, and primary rat astrocytes. *J Neuroimmunol.* 1993; 47(2):123–132. [PubMed: 7690370]
47. Yusa S, Catina TL, Campbell KS. SHP-1- and phosphotyrosine-independent inhibitory signaling by a killer cell Ig-like receptor cytoplasmic domain in human NK cells. *J Immunol.* 2002; 168(10):5047–5057. [PubMed: 11994457]
48. Zhang H, Bennett JL, Verkman AS. Ex vivo spinal cord slice model of neuromyelitis optica reveals novel immunopathogenic mechanisms. *Ann Neurol.* 2011; 70(6):943–954. [PubMed: 22069219]

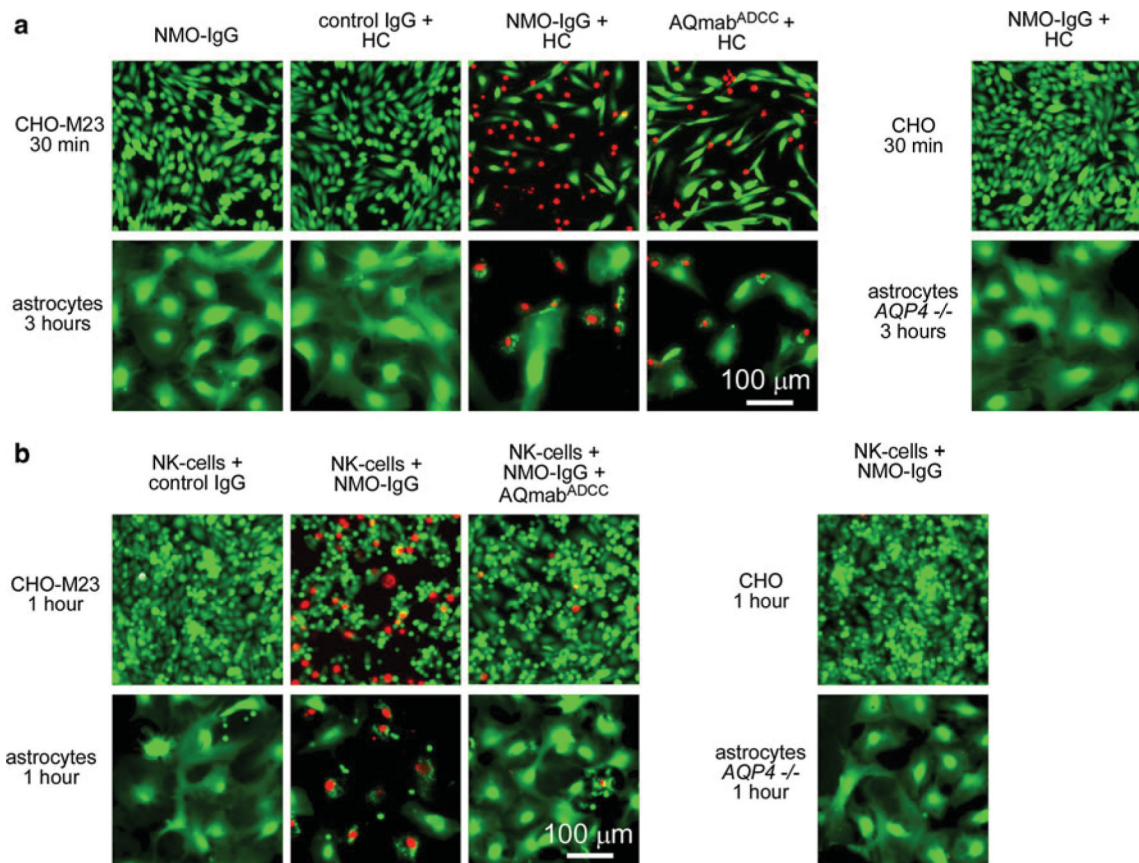


Fig. 1. NMO-IgG-dependent cytotoxicity in AQP4-transfected CHO cells and primary cultures of mouse astrocytes. **a** Fluorescence micrographs showing live/dead (*green/red*) staining of CHO cells expressing AQP4-M23 (CHO-M23) and mouse primary astrocyte cultures after incubation for indicated times with human complement (HC, 10 %) together with control (non-NMO) IgG or NMO-IgG or AQmab^{ADCC} (each 20 μ g/mL). **b** Fluorescence micrographs showing live/dead staining of cells incubated with NK-cells (NK-cell:target cell ratio of 20:1) and control IgG or NMO-IgG (20 μ g/mL) and/or AQmab^{ADCC} (200 μ g/mL).

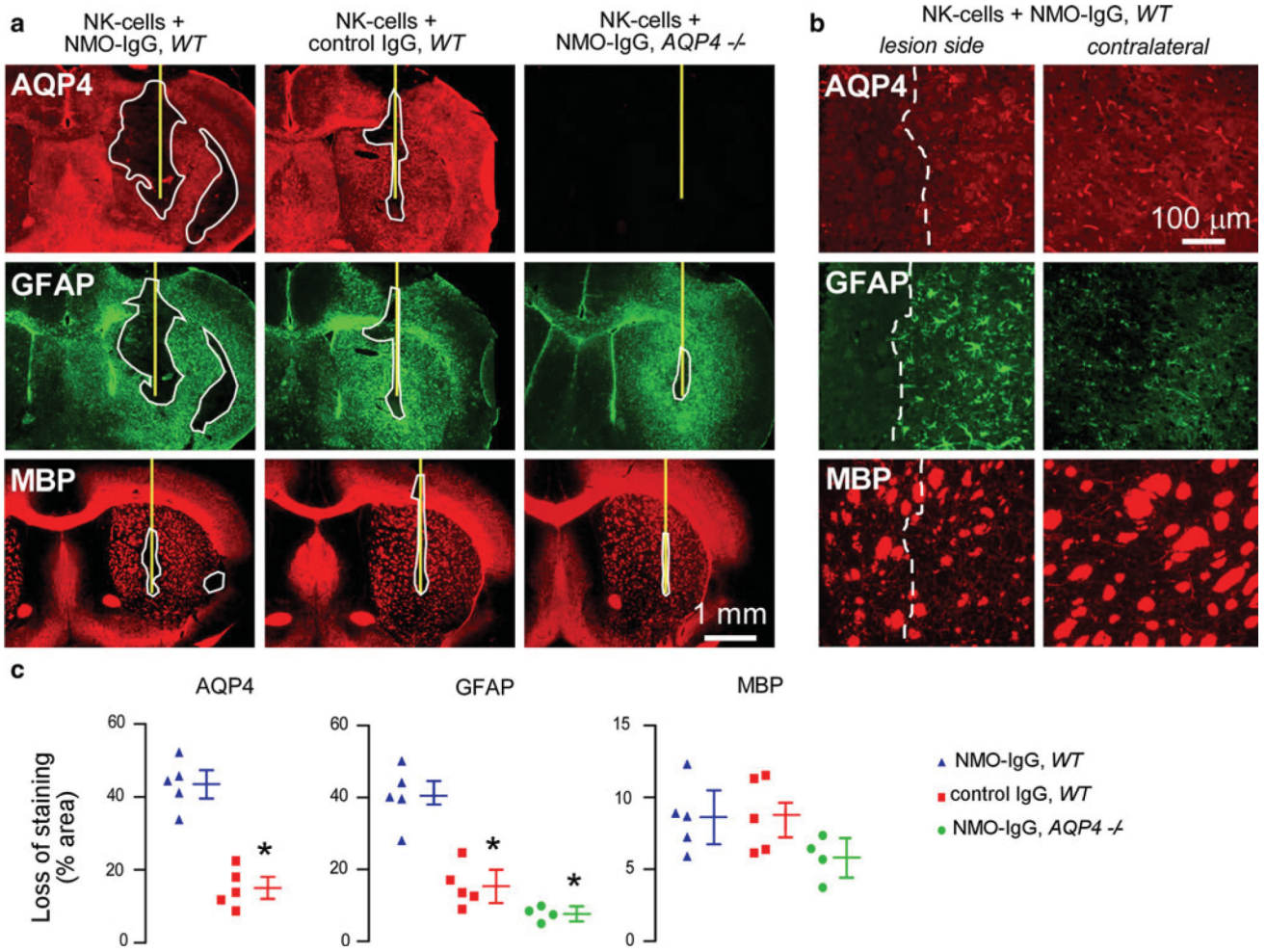


Fig. 2. Intracerebral injection of NMO-IgG and NK-cells causes loss of AQP4 and GFAP but not of myelin. **a** Brains of wild type (*WT*) and AQP4 deficient (*AQP4*^{-/-}) mice were injected with NK-cells (10^6 cells) and NMO-IgG or control IgG ($4 \mu\text{g}$). The mice were killed 4 days after injection and brain sections were immunostained for AQP4, GFAP and myelin (*MBP*). *Yellow line* represents the needle tract. *White line* shows the area of loss of immunoreactivity. Data are representative of four or five mice per group. **b** Higher magnification of *WT* mouse brain injected with NK-cells and NMO-IgG. Areas to the *left* of *white dashed line* show loss of AQP4 and GFAP but preservation of myelin. Contralateral (non-injected) hemispheres are shown (right). **c** Areas of loss of AQP4, GFAP and MBP immuno-reactivity (mean \pm SE, * $P < 0.01$ compared with *WT* mice injected with NK-cells and NMO-IgG)

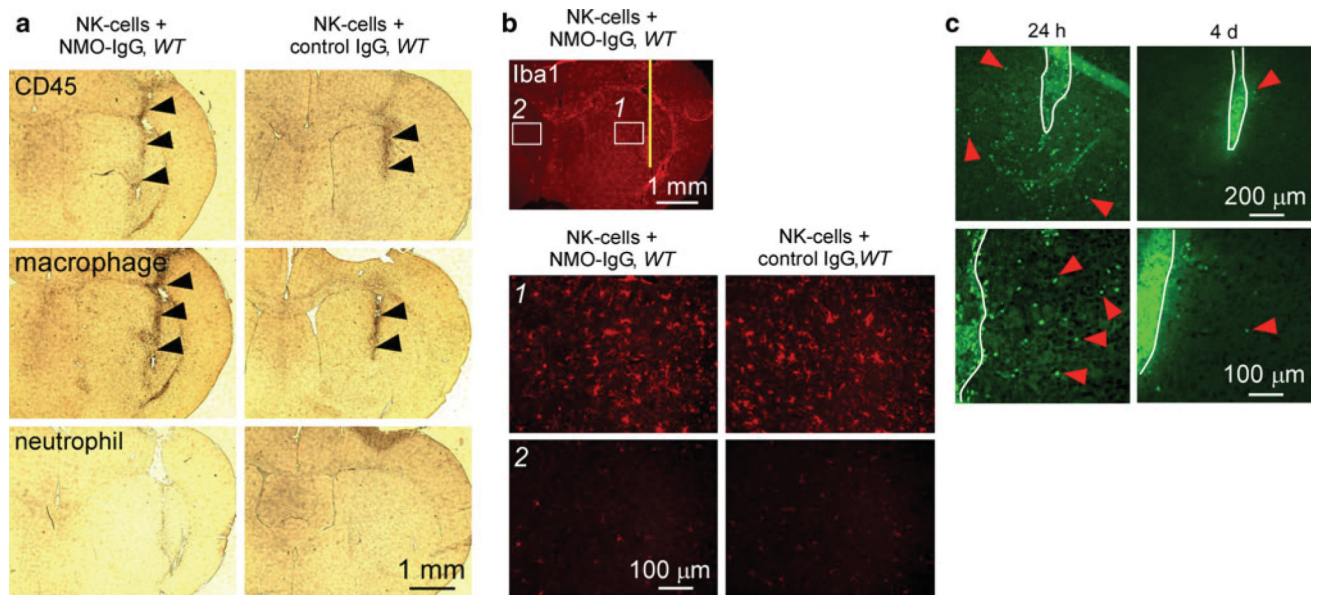


Fig. 3. Intracerebral injection of NMO-IgG and NK-cells causes minimal inflammation. **a** Immunohistochemistry showing CD45-positive cell infiltration in the needle tract (*black arrowheads*) of WT mice injected with NMO-IgG or control IgG. Most infiltrating cells were positive for a macrophage marker but negative for a neutrophil marker. **b** Sections stained for microglia marker Iba1 showing microglial activation around the needle tract (labeled 1) in mice injected with NK-cells and NMO-IgG or control IgG compared to contralateral hemisphere (labeled 2). **c** Fluorescence micrographs of GFP-NK-cells 24 h and 4 days after intracerebral injection. *White line* represents the needle tract. *Red arrowheads* indicate infiltrating NK-cells in brain parenchyma. Micrographs at the bottom are a higher magnification of the sections at the top

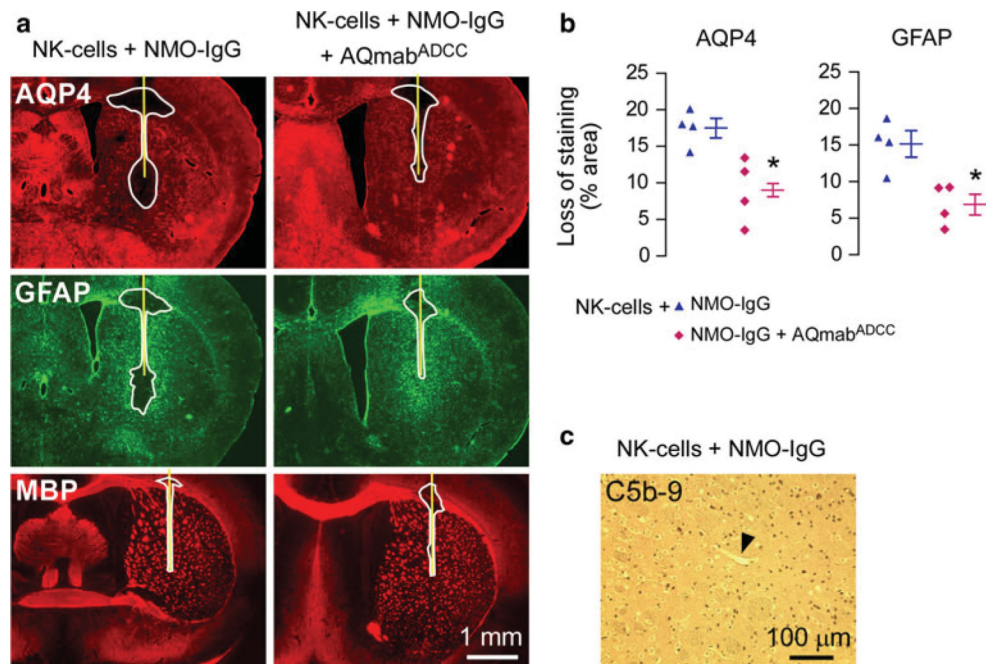


Fig. 4. Lesions following intracerebral injection of NMO-IgG and NK-cells are mediated by ADCC. **a** Brains of wild-type mice were injected with NK-cells (10^6 cells) and NMO-IgG ($1 \mu\text{g}$) or coinjected with NMO-IgG and an excess of AQmab^{ADCC} ($5 \mu\text{g}$). *Yellow line* represents the needle tract. *White line* shows the area of loss of immunoreactivity. Data are representative of four mice per group. **b** Quantification of areas of loss of AQP4 and GFAP immunoreactivity (mean \pm SE, $*P < 0.05$ compared with mice injected with NK-cells and NMO-IgG). **c** C5b-9 staining of brain injected with NK-cells and NMO-IgG showing absence of complement activation. *Arrowhead* points to a brain vessel

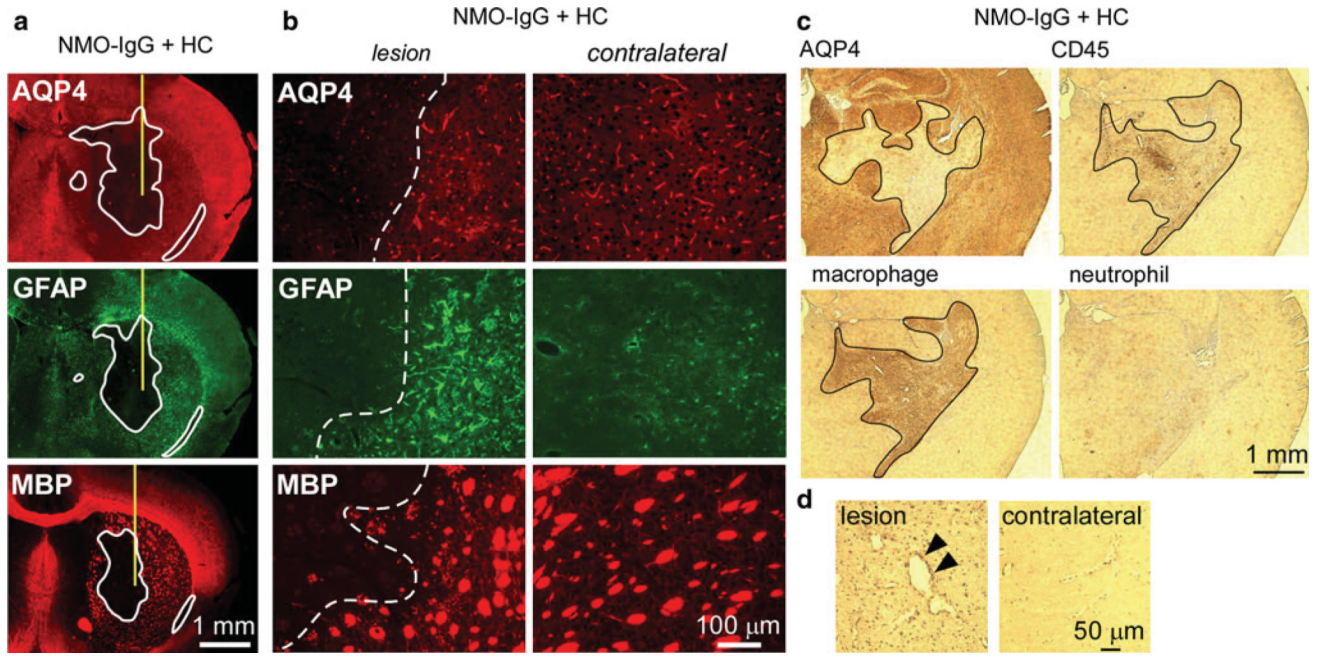


Fig. 5. Intracerebral injection of NMO-IgG and human complement produces demyelination and marked inflammation. **a** Brains were injected with NMO-IgG (0.4 μ g) and human complement (3 μ L) and stained for AQP4, GFAP and MBP. *Yellow line* represents the needle tract. *White line* shows areas of loss of immunoreactivity. Data are representative of four different mice. **b** Higher magnification of the sections shown in **a**. Areas to the *left* of *white dashed lines* show loss of AQP4, GFAP and myelin. Contralateral (non-injected) hemispheres are shown for comparison. **c** Same experiment as in **(a)** and **(b)**, showing marked infiltration of CD45-positive cells in the area of AQP4 loss. Most of the infiltrating cells are positive for a macrophage marker but negative for a neutrophil marker. *Black line* outlines the lesion. **d** C5b-9 staining in lesion and in contralateral hemisphere. *Arrowheads* indicate perivascular complement deposition

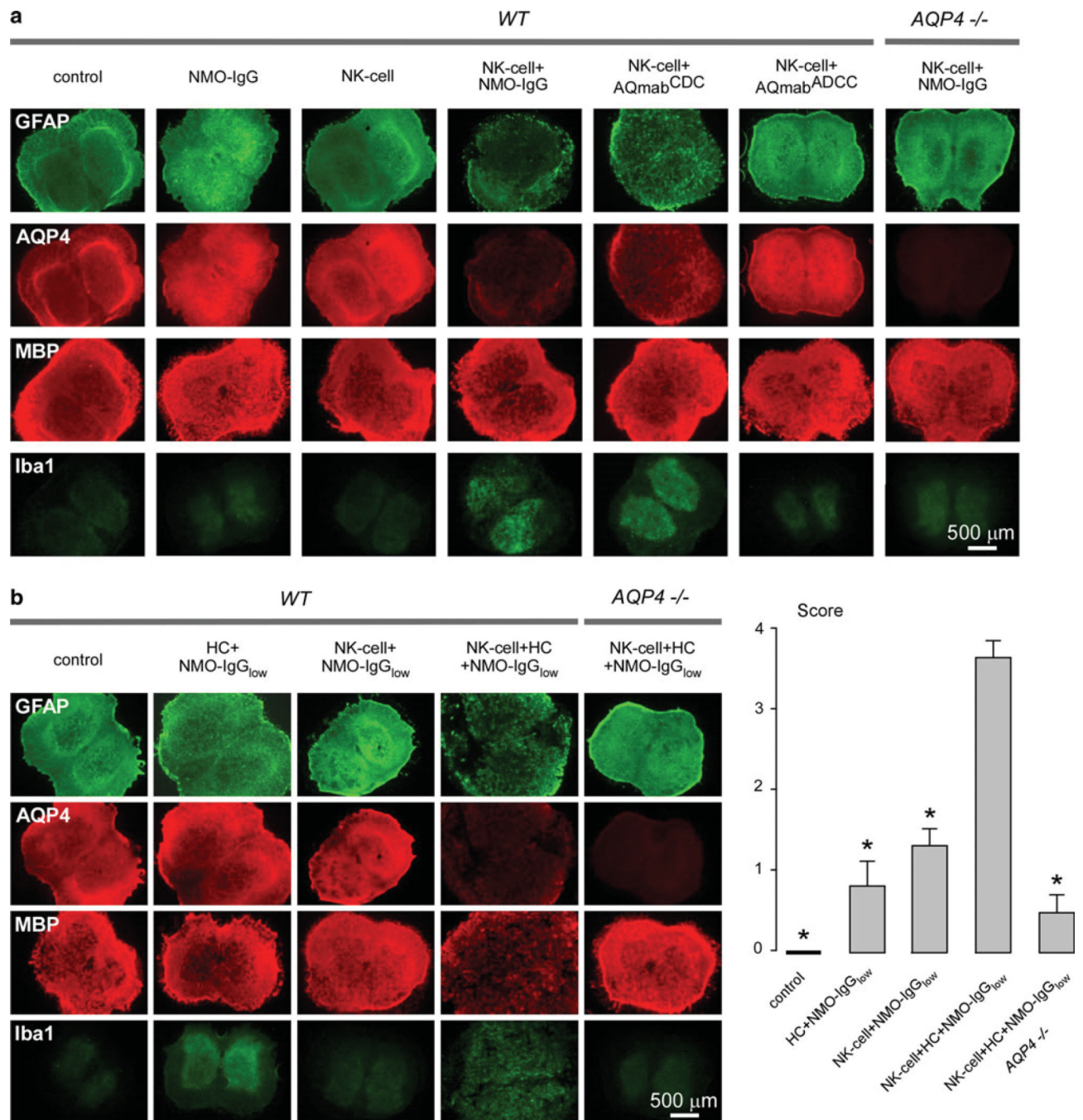


Fig. 6. NK-cells exacerbate NMO lesions produced by NMO-IgG and complement in an ex vivo spinal cord slice culture model. **a** Immunofluorescence of GFAP, AQP4, MBP and Iba1 in spinal cord slice cultures from wild type (WT) and *AQP4*^{-/-} mice incubated with NMO-IgG, AQmab^{CDC} or AQmab^{ADCC} (each 10 μ g/mL) and/or NK-cells (10^6 /well). *Control* indicates no NMO-IgG or NK-cells. **b** Same staining as in (a) of spinal cord slice cultures incubated with NK-cells (10^6 /well) and/or human complement (HC, 5 %) and/or submaximal NMO-IgG (NMO-IgG_{low}, 3 μ g/mL) (*left*). Scoring of NMO lesions (mean \pm SE, 6–8 slices per condition, **P* < 0.001 compared with NK-cell + HC + NMO-IgG_{low}, WT) (*right*)